Materials Science and Engineering A 527 (2010) 6028–6032

Contents lists available at ScienceDirect

Materials Science and Engineering A

journal homepage: www.elsevier.com/locate/msea

Further evidence of grain boundary internal friction in bicrystals

W.B. Jiang, Q.P. Kong*, P. Cui

Key Laboratory of Materials Physics, Institute of Solid State Physics, Chinese Academy of Sciences, Hefei 230031, PR China

ARTICLE INFO

Article history:
Received 20 May 2010
Accepted 28 May 2010

Keywords:
Grain boundary
Internal friction
Bicrystal
Aluminum

ABSTRACT

In order to further confirm the origin of grain boundary (GB) internal friction peak in bicrystals, the effect of GB density (i.e., GB area in unit volume of specimen) on the internal friction peak in pure aluminum is studied. It is found that the increment of GB density leads to a proportional increment of the peak height (or relaxation strength), while the activation parameters remain unchanged. The results further confirm that the observed internal friction peak in bicrystals is induced by the GB, rather than lattice dislocations in grain interior. By analyzing the stress components acting on the GB plane in bicrystals, the internal friction peak is interpreted by stress induced GB sliding. The restoring force to sliding is assumed due to the faceted junctions or steps in GBs.

© 2010 Elsevier B.V. All rights reserved.

1. Introduction

The grain boundary (GB) internal friction peak was first observed by Kê [1] in polycrystalline Al, and later also observed in many other polycrystalline materials [2–15]. The peak appears in the polycrystals, but disappears in the single-crystals, indicating that the peak is induced by GB relaxation. Its behavior and possible mechanisms were extensively investigated, but the detailed mechanism has not been clearly clarified.

Since the data of a polycrystal involve mixed contributions of different types of GBs which exhibit distinctive structure and property [16,17], in order to clarify the mechanism of the GB peak, the study of individual GB in bicrystals is necessary. There were a few studies on the internal friction in bicrystals of Cu and Al [5,18–20], but the information of the internal friction in bicrystals with different types of GBs were lacking.

In recent years, we have systematically studied the internal friction of pure aluminum bicrystals containing ⟨1 0 0⟩, ⟨1 1 2⟩, ⟨1 1 1⟩ tilt GBs and ⟨1 1 1⟩ twist GBs with a wide variety of misorientations [21–26]. It was found that a substantial internal friction peak appears in the bicrystals, but it disappears in the adjoining single-crystals. Since the bicrystals and the adjoining single-crystals are grown with the same history, it is evident that the peak observed in the bicrystals is induced by the GB. The activation parameters, the coupling effect and compensation effect involved in GB relaxation have been investigated in detail [23–26].

In order to further examine the origin of the internal friction peak in bicrystals, the present paper investigates the effect of GB density (i.e., GB area in unit volume of specimen) on the peak height (or relaxation strength). The usual procedure to study the effect of GB density in polycrystals is by changing the GB area (or the grain size) in a given specimen volume. But for the bicrystals, it is more convenient to investigate the effect of GB density by changing the specimen volume without changing the GB area. The results further confirm our previous conclusion that the observed internal friction peak is induced by GB relaxation. In addition, by analyzing the stress components acting on the GB plane in the bicrystals, the internal friction peak is interpreted by stress induced GB sliding, while the restoring force to sliding is assumed due to the faceted junctions or steps in GBs.

2. Experimental results

The internal friction as a function of temperature was measured by forced vibration method at constant excitation strain amplitude 1×10^{-5} in an automatic inverted torsion pendulum. The temperature changing rate during heating or cooling was about 2 K/min. The detailed experimental procedures were described elsewhere [21–26].

The bicrystals were prepared by Bridgman method with 99.999% pure Al. The bicrystals were characterized to have a planar symmetrical GB. The dimensions of our usually used bicrystals were 50 mm in length, 4 mm in width, and 2 mm in thickness as shown in Fig. 1(a). The specimens with cross section 4 mm × 2 mm are named specimen type 1.

For increasing the GB density, we reduced the width from 4 mm to 2 mm by electro-discharge cutting off 1 mm from each side of lateral surfaces of the specimen type 1, while the length and thickness of specimen were not changed, as shown in Fig. 1(b). The boundary area was still 50 mm × 2 mm. The spec-

* Corresponding author. Tel.: +86 551 5591427; fax: +86 551 5591434.
E-mail address: qpkong@issp.ac.cn (Q.P. Kong).

0921-5093/$ – see front matter © 2010 Elsevier B.V. All rights reserved.
doi:10.1016/j.msea.2010.05.091

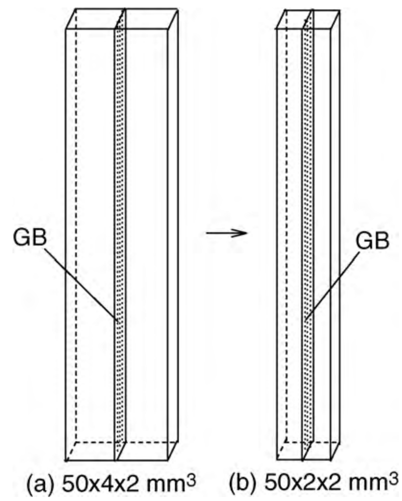

Fig. 1. Bicrystal dimensions:(a) 50 mm × 4 mm × 2 mm (specimen type 1). and (b) 50 mm × 2 mm × 2 mm(specimen type 2). The shaded area is grain boundary.

imens with cross section 2 mm × 2 mm are named specimen type 2.

We can see that by reducing the specimen volume, the GB density of the specimen type 2 is doubled compared to the specimen type 1, while the GB area and its configuration were not changed.

Figs. 2 and 3 show the examples of internal friction peak for the specimen types 1 and 2 in bicrystals with ⟨1 0 0⟩ 9.3° and ⟨1 1 1⟩ 34.9° tilt GBs respectively (at 1 Hz). The net peak (denoted by solid line) is obtained by subtracting the background (denoted by dashed line, which is assumed to exponentially increase with temperature) from the experimental data by a fitting procedure. It can be seen from the figures that when the GB density is doubled, the apparent and the net peak heights are also nearly doubled, while the peak temperatures are not changed.

Fig. 4 shows the internal friction peak for the specimen types 1 and 2 in the bicrystal with ⟨1 1 1⟩ 10.8° tilt GB at different frequencies. It can be seen from Fig. 4 that the peak shifts to higher temperature at higher frequency similarly for both types of specimens.

Based on the assumptions that the relaxation obeys the Debye relaxation function, and without considering the interaction between relaxing species, the peak occurs at the following

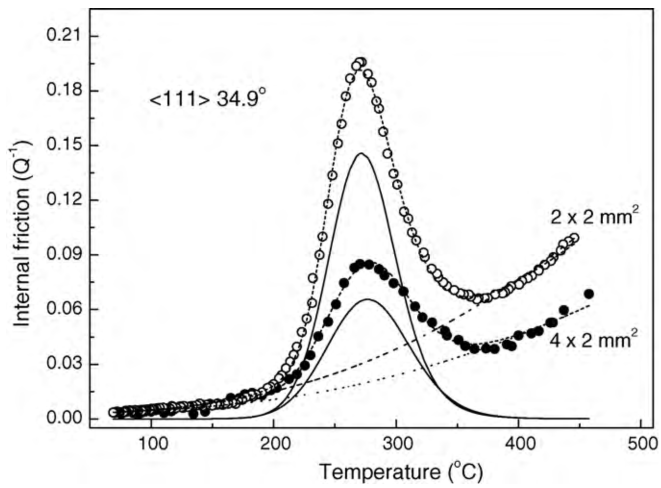

Fig. 3. Comparison of the internal friction peak for the specimen types 1 and 2 in bicrystals with ⟨1 1 1⟩ 34.9° tilt GB at 1 Hz.

condition [3]:

$$\omega\tau = \omega\tau_0 \exp\left(\frac{H}{kT_p}\right) = 1 \qquad (1)$$

where τ is the relaxation time, τ_0 is the pre-exponential factor, ω is the circular frequency ($\omega = 2\pi f$, f is the measuring frequency), H is the apparent activation enthalpy, k is the Boltzmann constant, and T_p is the absolute temperature of the net peak. With the net peak temperatures at different frequencies, the apparent activation enthalpy H and pre-exponential factor τ_0 can be evaluated.

Fig. 5 shows the Arrhenius plots (natural logarithm of circular frequency ω versus the reciprocal of net peak temperature $1/T_p$) for the specimen types 1 and 2 in bicrystal with ⟨1 1 1⟩ 10.8° tilt GB. It can be seen that the data of the two types of specimens are almost fallen on the same straight line.

The net peak height Q_m^{-1}, relaxation strength Δ, and apparent activation parameters for the specimen types 1 and 2 are listed in Table 1. The relaxation strengths Δ are evaluated with the net peak height Q_m^{-1} and the measured value of the distribution parameter of relaxation time β, as in the previous works [21,22].

One can see from Table 1 that the net peak heights Q_m^{-1} (or relaxation strengths Δ) for the specimen type 2 are nearly doubled compared to the specimen type 1. Both the ratios of Q_{m2}^{-1}/Q_{m1}^{-1} and Δ_2/Δ_1 are within the range of 2.0 (±0.2). But the activation

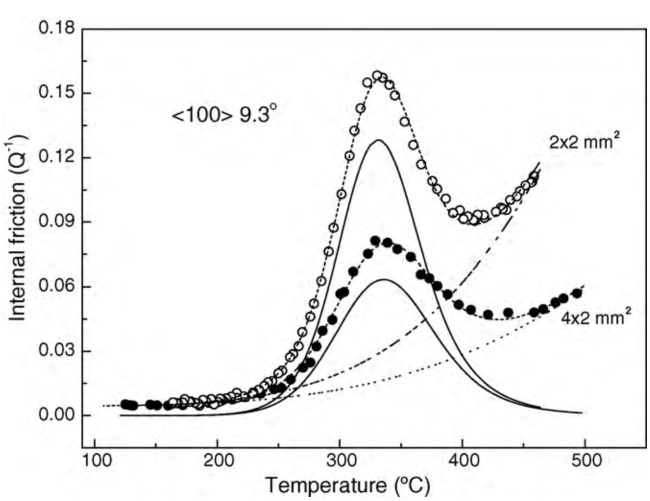

Fig. 2. Comparison of the internal friction peak for the specimen types 1 and 2 in bicrystals with ⟨1 0 0⟩ 9.3° tilt GB at 1 Hz.

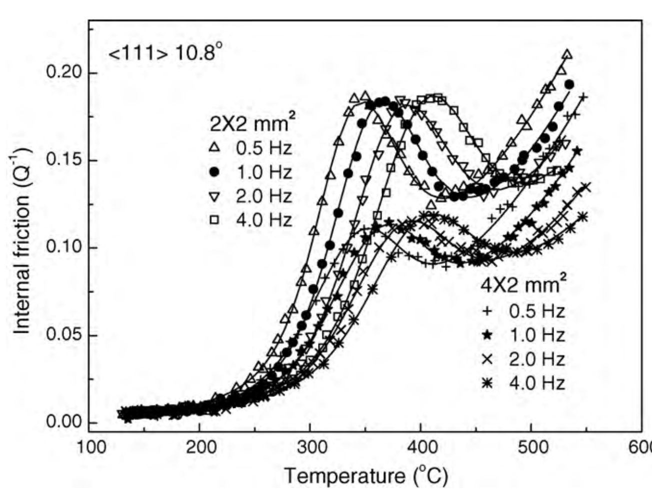

Fig. 4. The internal friction peak for the specimen types 1 and 2 in bicrystal with ⟨1 1 1⟩ 10.8° tilt GB at different frequencies.

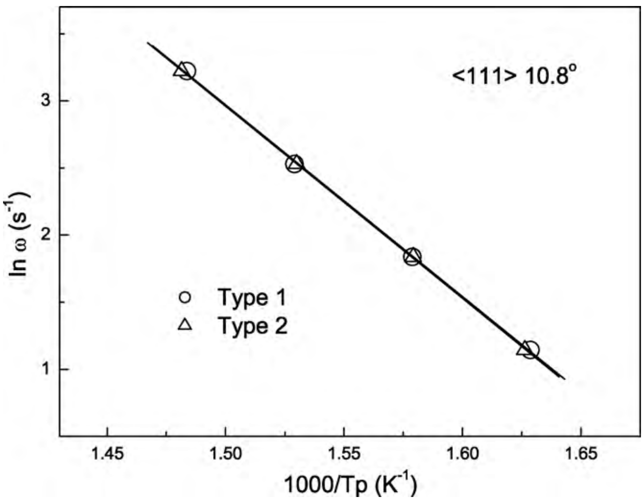

Fig. 5. The Arrhenius plots for the specimen types 1 and 2 in bicrystal with ⟨1 1 1⟩ 10.8° tilt GB.

parameters (H and τ_0) of the specimen types 1 and 2 are consistent with each other within experimental error, indicating that the mechanism of the peak does not change with the variation of GB densities.

The activation parameters in Table 1 will not be specifically explained here. As analyzed in our previous papers [23–26], the activation parameters of the low-angle tilt GBs (⟨1 0 0⟩ 9.3° and ⟨1 1 1⟩ 10.8°) can be explained by dislocation climb mechanism. By using the coupling model [27–30], the high activation enthalpy H of the high-angle ⟨1 1 1⟩ 34.9° tilt GB can be attributed to the coupling effect (or interaction) between relaxing species. After decoupling, the specific activation enthalpy H^* is evaluated to be ∼1.0 eV, which is probably related to the basic process of correlated motion in GB relaxation [23–26].

3. Discussion

3.1. On the dependence of peak height on GB density

The interesting finding in this study is that the increment of GB density leads to a proportional increment of internal friction peak height (or relaxation strength) in the bicrystals.

As well known, the internal friction is a measure of energy loss in vibration, which can be expressed by [2,3]

$$Q^{-1} = \frac{1}{2\pi}\frac{\Delta W}{W} \quad (2)$$

where ΔW is the energy loss in a cycle per unit volume of specimen, W is the maximum stored energy per unit volume of specimen.

For a specimen with volume V, the stored energy will be $W \times V$. If the observed internal friction peak is induced by GB relaxation in bicrystals, the energy loss for the peak will be proportional to the total GB area (A) in whole specimen. Thus, Eq. (2) can be re-written as

$$Q^{-1} = \frac{1}{2\pi}\frac{\Delta W_b}{W}\frac{A}{V} \quad (3)$$

where ΔW_b is the energy loss per unit area of GB in a cycle, and $(1/2\pi)(\Delta W_b/W)$ is a constant (with dimension of mm^3/mm^2) under the specific experimental condition.

It turns out from Eq. (3) that under the specific condition, the peak value of internal friction should be proportional to A/V, i.e., the GB density. Since the volume V_2 of the specimen type 2 is half as the volume V_1 of the specimen type 1, and the GB area (50 mm× 2 mm) is kept unchanged, the peak height (or relaxation strength) of the former should be twice as that of the latter.

The experimental results (Figs. 2–4 and Table 1) are in agreement with the consideration of energy loss due to GB relaxation. Hence it further confirms that the observed internal friction peak in the bicrystals is induced by the GB.

The results also exclude the possibility that the observed peak in bicrystals might be induced by the lattice dislocations in grain interior. If the internal friction peak were induced by lattice dislocations in grain interior, the energy loss ΔW should be related to the total dislocation length in unit volume of specimen. When the specimen volume changes, both energy loss ΔW and the stored energy W should change with the same proportion. Referring to Eq. (2), the reduction of specimen volume should not influence the peak height (or relaxation strength).

3.2. The stress induced GB sliding in the internal friction

The internal friction peak can be interpreted by stress induced GB sliding in the bicrystals. The bicrystals with cross section 4 mm× 2 mm or 2 mm× 2 mm are longitudinally aligned along the length (50 mm). The GB plane is normal to Y-axis and located in the middle part of bicrystal (see Fig. 6(a)). During internal friction measurement, the lower end is fixed, while the upper end is periodically twisted.

Consider the stress components acting on the planes of a cubic volume element containing the GB plane (see Fig. 6(b)). At the given condition, the shear stresses σ_{zx} and σ_{zy} are applied on the XOY planes. According to the equilibrium condition of elastic mechanics, the shear stress components σ_{xz} and σ_{yz} should also exist, which are equal in magnitude with σ_{zx} and σ_{zy} respectively, but different in acting plane and direction. In the current case, the normal stresses σ_{xx}, σ_{yy}, σ_{zz} and shear stresses σ_{xy}, σ_{yx} are zero.

The applied stress will result in the strain of the specimen. Below the so-called "equicohesive temperature" T_{eq} [31], the strength of GB is higher than that of grain, and the GB deforms with the matrix without separate sliding. But above T_{eq}, the strength of GB is lower than that of grain, and the viscous sliding of GB takes an important part in the total strain. Thus the effective shear stresses will result in torsion and sliding of the GB, the GB sliding is accompanied with GB torsion. The internal torsion is generally assumed to contribute negligibly to the strain energy [32]. Hence, from the consideration of energy dissipation, the GB internal friction is mainly induced by GB sliding, as generally recognized [1–4].

Table 1
The net peak height Q_m^{-1}, the ratio of Q_{m2}^{-1}/Q_{m1}^{-1}, the relaxation strength Δ, the ratio of Δ_2/Δ_1, the apparent activation enthalpy H and pre-exponential factor τ_0 for the specimen types 1 and 2 of pure Al bicrystals.

Bicrystal	Spec.Type	Q_m^{-1} (±0.005)	Q_{m2}^{-1}/Q_{m1}^{-1}	Δ (±0.02)	Δ_2/Δ_1	H (eV) (±0.05)	τ_0 (s)
9.3°⟨1 0 0⟩	1	0.063	2.0	0.17	1.8	1.31	$1.5 \times 10^{-12\pm1}$
	2	0.128		0.31		1.42	$2.2 \times 10^{-13\pm1}$
10.8°⟨1 1 1⟩	1	0.075	1.9	0.18	1.9	1.26	$1.6 \times 10^{-11\pm1}$
	2	0.141		0.35		1.23	$2.0 \times 10^{-11\pm1}$
34.9°⟨1 1 1⟩	1	0.066	2.2	0.31	1.9	1.82	$1.1 \times 10^{-18\pm1}$
	2	0.145		0.60		1.84	$1.8 \times 10^{-18\pm1}$

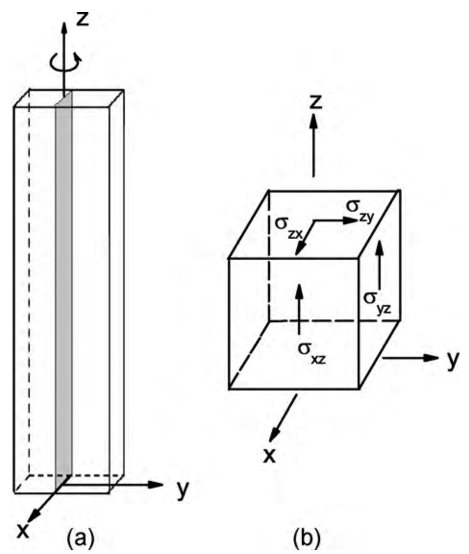

Fig. 6. The stress induced GB sliding in the internal friction: (a) the alignment of the bicrystals; and (b) the stress components.

Adopting the viscous sliding model [2,3], the contribution of GB sliding in total strain can be evaluated from the relaxation strength. In the internal friction measurement, the strain amplitude ε (10^{-5}) includes the elastic strain ε_0 and the anelastic strain ε_a (the latter is caused by GB sliding). In order to separate ε_a from the total strain ε, we use the following equation [2,3]

$$\Delta = \frac{M_U - M_R}{M_R} = \frac{\varepsilon_a}{\varepsilon_0} \tag{4}$$

where M_U and M_R are unrelaxed and relaxed moduli respectively. From Eq. (4), we have

$$\frac{\varepsilon_a}{\varepsilon_0 + \varepsilon_a} = \frac{\varepsilon_a}{\varepsilon} = \frac{\Delta}{1+\Delta} \tag{5}$$

The contribution of GB sliding in total strain $\varepsilon_a/\varepsilon$ evaluated from the relaxation strength by Eq. (5) are evaluated and listed in Table 2. The values of $\varepsilon_a/\varepsilon$ for specimen type 1 are 15–24%, and those of specimen type 2 are 24–38%.

For the internal friction peak to occur, the GB sliding in polycrystals was assumed to be restricted by grain edges and corners in anelastic internal friction [1–3]. Since there is no grain edge and corner in bicrystals, the restoring force to sliding should be searched in another way. Many evidences show that a GB is actually not smooth, but consists of numerous facets with orientations slightly deviated from the average GB plane [16,33,34]. The length of the facets is usually of the order of a few hundred nanometers to 1 μm. Thus the faceted junctions or steps in GBs may act as obstacles to block the GB sliding.

Based on assumptions of elastic accommodation and sinusoidal boundary shape, Raj and Ashby ever estimated the GB sliding displacement in internal friction of polycrystals, they derived the average GB sliding displacement [35]

$$\overline{U} = \frac{4(1-\nu^2)}{\pi^3}\frac{\lambda^3}{h^2}\frac{\tau_a}{E} \tag{6}$$

where λ is the wave length of boundary shape, h is the amplitude, τ_a is the shear stress, E is the Young's modulus, and ν is the Poissons ratio.

Assuming the facet junctions act as obstacles, the model and Eq. (6) of Raj and Ashby can also be applied to the faceted boundary in bicrystals. Based on the observations of faceted boundaries [16,33,34], we may assume the average facet size $\lambda \approx 500$ nm, and $h = 2$–3 nm. Since E=2(1+ν)G (G is shear modulus) and $\tau_a/G = 10^{-5}$, $\tau_a/E = 10^{-5}/[2(1+\nu)]$. Inserting these values and $\nu = 0.34$ into Eq. (6), we obtain that the average GB sliding displacement in the bicrystals $\bar{U}$ is approximately equal to 6–13 nm, which is a little higher than but still near to that (≈5 nm) estimated in polycrystals [35].

Table 2
The contribution of GB sliding in total strain $\varepsilon_a/\varepsilon$.

Bicrystal	Specimen type	Relaxation strength, Δ	$\varepsilon_a/\varepsilon$
9.3°⟨1 0 0⟩	1	0.17	15%
	2	0.31	24%
10.8°⟨1 1 1⟩	1	0.18	15%
	2	0.35	26%
34.9°⟨1 1 1⟩	1	0.31	24%
	2	0.60	38%

4. Conclusions

(1) The effect of GB density (i.e., GB area in unit volume of specimen) on the internal friction peak in pure aluminum bicrystals is studied by changing the specimen dimension but not changing the GB area and GB configuration. It is found that the increment of GB density leads to a proportional increment of the peak height (or relaxation strength), while the activation parameters remain unchanged.
(2) The experimental results are in agreement with the consideration of energy loss by GB relaxation, further confirming that the observed internal friction peak in the bicrystals is induced by the GB, rather than lattice dislocations in grain interior.
(3) By analyzing the stress components acting on the GB plane, the internal friction peak is interpreted by stress induced GB sliding in bicrystals. The restoring force to sliding is assumed due to the faceted junctions or steps in GBs.

Acknowledgment

The authors are grateful to the National Natural Science Foundation of China (under Grants 10674136 and 10804108) for financial support.

References

[1] T.S. Kê, Phys. Rev. 71 (1947) 533–546.
[2] T.S. Kê, Metall. Mater. Trans. A 30 (1999) 2267–2295.
[3] A.S. Nowick, B.S. Berry, Anelastic Relaxation in Crystalline Solids, Academic Press, New York, 1972.
[4] H. Gleiter, B. Chalmers, High Angle Grain Boundaries, Pergamon Press, Oxford, 1972.
[5] K. Iwasaki, Phys. Stat. Sol. A 81 (1984) 485–496.
[6] T.S. Kê, P. Cui, C.M. Su, Phys. Stat. Sol. A 84 (1984) 157–164.
[7] T.S. Kê, B.S. Zhang, Phys. Stat. Sol. A 96 (1986) 515–525.
[8] Q.P. Kong, Y. Dai, Phys. Stat. Sol. A 118 (1990) 431–439.
[9] F. Povolo, B.J. Molinas, Nuovo Cimento 14 D (1992) 287–332.
[10] B.J. Molinas, F. Povolo, Mater. Sci. Forum 119–211 (1993) 39–48.
[11] W. Benoit, Mater. Sci. Forum 366–368 (2001) 291–314.
[12] Q.P. Kong, B. Cai, G. Gottstein, J. Mater. Sci. 36 (2001) 5429–5434.
[13] Y. Shi, B. Cai, Q.P. Kong, P. Cui, G. Gottstein, J. Mater. Sci. 38 (2003) 1895–1899.
[14] W. Benoit, Mater. Sci. Eng. A 370 (2004) 12–20.
[15] B.M. Darinskii, Yu E. Kalinin, D.S. Sajko, Solid State Phenom. 115 (2006) 73–86.
[16] A.P. Sutton, R.W. Balluffi, Interfaces in Crystalline Materials, Oxford University Press, Oxford, 1995.
[17] G. Palumbo, K.T. Aust, in: D. Wolf, S. Yip (Eds.), Materials Interface, Chapman and Hall, London, 1992, p. 190.
[18] M. Kato, T. Mori, Philos. Mag. A 68 (1993) 939–949.
[19] L.X. Yuan, T.S. Kê, Phys. Stat. Sol. A 154 (1996) 573–581.
[20] X.G. Guan, T.S. Kê, J. Alloys Compd. 211–212 (1994) 480–483.
[21] Y. Shi, P. Cui, Q.P. Kong, W.B. Jiang, M. Winning, Phys. Rev. B 71 (2005) 060101.
[22] W.B. Jiang, P. Cui, Q.P. Kong, Y. Shi, M. Winning, Phys. Rev. B 72 (2005) 174118.
[23] Y. Shi, W.B. Jiang, Q.P. Kong, P. Cui, Q.F. Fang, M. Winning, Phys. Rev. B 73 (2006) 174101.
[24] Q.P. Kong, W.B. Jiang, Y. Shi, P. Cui, Q.F. Fang, M. Winning, Mater. Sci. Eng. 521–522 (2009) 128–133.

[25] W.B. Jiang, Q.P. Kong, D.A. Molodov, G. Gottstein, Acta Mater. 57 (2009) 3327–3331.
[26] W.B. Jiang, Q.P. Kong, P. Cui, F.Q. Fang, D.A. Molodov, G. Gottstein, Philos. Mag. 90 (2010) 753–764.
[27] K.L. Ngai, A.K. Jonscher, C.T. White, Nature 277 (1979) 185–189.
[28] Y.N. Wang, M. Gu, L.H. Sun, K.L. Ngai, Phys. Rev. B 50 (1994) 3525–3531.
[29] L.B. Magalas, Solid State Phenom. 89 (2003) 1–22.
[30] X.P. Wang, Q.F. Fang, Phys. Rev. B 65 (2002) 064304.
[31] H. Conrad, in: J.E. Dorn (Ed.), Mechanical Behavior of Materials at Elevated Temperatures, McGraw-Hill Book Company, Inc., New York, 1961, p. 218.
[32] J.P. Hirth, J. Lothe, Theory of Dislocations, John Wiley & Sons, Inc., New York, 1982, p. 31.
[33] Q. Jin, S.W. Chan, J. Mater. Res. 17 (2002) 323–335.
[34] J.C. Hamilton, D.J. Siegel, I. Daruka, F. Leonard, Phys. Rev. Lett. 90 (2003) 246102.
[35] R. Raj, M.F. Ashby, Metall. Trans. 2 (1971) 1113–1127.